International Journal of Engineering

Image Restoration by Projection onto Convex Sets with Particle Swarm Parameter Optimization

A. Rashno*[a], S. Fadaei[b]

[a] Department of Computer Engineering, Engineering Faculty, Lorestan University, Khorramabad, Iran
[b] Department of Electrical Engineering, Faculty of Engineering, Yasouj University, Yasouj, Iran

P A P E R   I N F O

A B S T R A C T

Image restoration is the operation of obtaining a high-quality image from a corrupt/noisy image and is widely used in many applications such as Magnetic Resonance Imaging (MRI) and fingerprint identification. This paper proposes an image restoration model based on projection onto convex sets (POCS) and particle swarm optimization (PSO). For this task, a number of convex sets are used as constraints and images are projected to these sets iteratively to reach restored image. Since relaxation parameter in POCS has a significant effect on restoration results, PSO is developed to find the best value for this parameter to be used in restoration process. The proposed scheme for image restoration is evaluated on three popular images with 4 configurations of noise, compared with 5 competitive restoration models. Results demonstrate that the proposed method outperforms other models in 32 out of 48 cases in images with different noise configurations with respect to relative error, ISNR, MAE and MSE measures.

1. INTRODUCTION

Recovery a high-quality image from its degraded version, well-known as image restoration, is a fundamental and difficult problem in image processing field which is applicable in many fields such as Magnetic Resonance Imaging, identification of fingerprint, astronomy and so on [1]. As we know, the accuracy of image processing algorithms is depended to the quality of the input image, so, image restoration problem which improves the quality of image plays an important role in this field. To do this, variety of algorithms are introduced.

Li et al. [2] proposed an image restoration approach for fingerprint by manipulating nonlocal Cahn–Hilliard equation. In this paper, the damaged part is considered and the nonlocal CH equation is solved to restore the fingerprint image. A Generative Adversarial Network (GAN) can be used to eliminate the overfitting problem among the recent networks and then improve the image restoration performance [3]. A conjugate gradient

algorithm is presented by Cao and Wu [4] to improve image restoration which possesses three properties: satisfaction of descent property; establishment of the trust region feature; convergence for nonconvex functions. A deep CNN referred as CU-Net is presented by Deng and Dragotti [5] to address the general multi-modal image restoration and multi-modal image fusion problems. The proposed network can split the common information automatically which can be shared among different modalities.

An extend and improved version of the Expected Patch Log Likelihood (EPLL) algorithm is proposed by Papyan and Elad [6] in which a multi-scale prior extracted from the target image is considered. Pang et al. [7] introduced a new model for image restoration based on minimizing surface regularization which is related to the classical ROF (Rudin, Osher and Fatemi) model [8]. By considering the support and sparsity prior together, a new method is presented by He et al. [1]. Also, the proximal alternating adaptive hard thresholding (PAAHT) algorithm is proposed to solve nonconvex

Corresponding Author Institutional Email: rashno.a@lu.ac.ir
(A. Rashno)

nonsmooth optimization problem. To address the problems of Rotating Synthetic Aperture (RSA) imaging system, an image restoration approach is presented by Zhi et al. [9]. In this work, the characteristics of image degradation analysis and mutual information are combined.

Zhang [10] has introduced a new restoration method by implementation of Expectation-Maximation algorithm using wavelet transform. A novel scheme is presented by Tanikawa et al. [11] based on weighted averaging of two images with different blur and noise artifacts. Indeed, the blur and noise artifacts are removed from the image by merging two degraded images. Although it is assumed that the image transformation be known in many methods, the transformation from the degraded image is estimated by Ševčík et al. [12] and this assumption is relaxed. A novel restoration algorithm is presented by Hu et al. [13] to remove both Gaussian noise and stripping artifacts. Some practical methods were proposed by Dar et al. [14] for image restoration when the degradation is an arbitrary form of known linear operator. Using the entropy constraint and the projection onto convex set algorithm, an effective restoration method based on super resolution is presented by Li et al. [15].

In case of the data with different scales, construction of a low-rank tensor is needed, so Lu et al. [16] proposed a model based on multi-band filters which are guided using low-rank tensor. An edge detection based on wavelet frame model is introduced by Choi et al. [17] to conduct image restoration by assuming that the image is a smooth function. Motohashi et al. [18] proposed a new method based on blind deconvolution to estimate the point spread function and improve the performance of restoration. A learning framework method based on Bayesian dictionary is introduced by Liu et al. [19] which the performance of image restoration is improved using the beta process of nonlocal structures. Image restoration is handled by using an effective neural network by Gou et al. [20]. A fitness-based multi-role particle swarm optimization was proposed Xia et al. [21]. Finally, convergence speed of a novel binary PSO was improved by fitness-based acceleration coefficients [22]. A new framework for image enhancement is proposed by Iravani and Ezoji [23] using optimization theorem. The quality of the image was improved by Tang et al. [24], Lin and Feng [25] based on image denoising. Mortezaei et al. [26] introduced an adaptive un-sharp masking algorithm to enhance image quality. An adaptive image dehazing approach was proposed by Azari Nasrabad et al. [27] based on dark channel prior. A higher resolution image was produced by Seyyedyazdi and Hassanpour [28, 29] using super resolution processing.

The main contributions of this paper are summarized as follows: 1) Image restoration is modeled by finding a common point to satisfy a set of convex sets constraints in Hilbert space, referred as projection onto convex sets (POCS); 2) In POCS, importance of relaxation parameter is investigated during restoration process and it is shown that how this parameter affects restoration quality; 3) A new schema for velocity update is proposed by first dividing particles to two groups based on their fitness and then applying velocity update rules to each group separately; 4) A new method for assigning particles inertia weight is finally proposed to control the process of exploration and exploitation.

The rest of the paper is organized as follows: Image restoration by projecting onto convex sets and particle swarm optimization algorithm are explained in sections 2 and 3. Section 4 introduces the proposed method. Implementation setup and results are reported in sections 5 and 6, respectively. Computation complexity of the fitness function in optimization process is discussed in section 7. Finally, the paper is concluded in section 8.

2. IMAGE RESTORATION BY PROJECTION ONTO CONVEX SETS

In the case of finding a common point f which satisfies a set of constraints as convex sets in Hilbert space R, POCS could be applied and used as follows:

$$f \in C = \cap_{i=1}^{m} C_i \tag{1}$$

where m is the number of convex sets and C_i is the ith closed convex set which is corresponding to ith constraint. The intersection vector f is found by successive projection onto convex sets started from any vector in R as initial guess f^0 with the following operator:

$$f^{t+1} = P_{C_m} P_{C_{m-1}} \dots P_{C_1} f^t \tag{2}$$

which means f at iteration $t+1$ is computed from projection of f at iteration t to convex set C_i by projection operator P_{C_i}.

It is worth mentioning that these projections converge to intersection point f in case that the intersection of convex sets is non-empty. The noise-free image restoration can be modeled as the following linear equation:

$$g = Hf \tag{3}$$

where H is PSF matrix, f is noise-free image and g is the degraded image. Each line of g is an equation that could be represented by a convex set. So, Equation (3) can be solved by POCS algorithms. Row-Action Projection (RAP) is a POCS method for solving Equation (3) [30]. The RAP equation which converges to intersection of hyperplanes is defined as follows [31]:

$$f^{(k+1)} = f^{(k)} + \lambda \frac{g_p - h_p^t f^{(k)}}{\|h_p\|^2} \tag{4}$$

where g_p and h_p^t are the pth element and pth row of vector g and matrix H respectively. λ is the relaxation parameter which is the main contribution of this paper. Since iteration index p is computed by $p = k(mod\ AB)$, each row is used multiple times in the iterations of the algorithm.

RAP can be reformulated for 2-D images. Each pixel of blurred image corresponds to Equation (4). The RAP in 2-dimensional space is proposed by the following equations.

$$\hat{f}^{(k+1)} = \begin{cases} \hat{f}^{(k)}(m,n) + \lambda \frac{\epsilon(i,j)}{\|h(i,j)\|^2} h(i-m, j-m), \\ \qquad \text{for } \hat{f}^{(k)}(m,n) \epsilon S_{h(i,j)} \\ \hat{f}^{(k)}(m,n), \qquad\qquad otherwise \end{cases} \quad (5)$$

where,

$$\epsilon(i,j) = g(i,j) - \sum_{m,n \epsilon S_{h(i,j)}} h(i-m, j-n; i,j)\hat{f}^{(k)}(m,n) \quad (6)$$

$$\|h(i,j)\|^2 = \sum_{m,n \epsilon S_{h(i,j)}} h(m,n; i,j)^2 \quad (7)$$

in Equations (6) and (7), $S_{h(i,j)}$ is the support of PSF centered at $g(i,j)$. At each iteration, projection operator is local which require only the pixels inside a window around each pixel [31, 32]. The lower and upper bounds for image pixels during iteration of restoration process are controlled by Limited Amplitude (LA) set as following:

$$C_{LA} = \{s: s \epsilon S \ and \ \alpha \le s(k,l) \le \beta \ \forall \ k,l \ \in \Omega\} \quad (8)$$

where Ω is the support region of the image, α and β are the upper and lower bounds, respectively and S is the Hilbert space. So, the projection operator can be defined as follows:

$$P_{C_{LA}}x(k,l) = \begin{cases} \alpha, & x(k,l) < \alpha \\ x(k,l), & \alpha \le x(k,l) \le \beta \\ \beta, & x(k,l) > \beta \end{cases} \quad (9)$$

In this transformation, bound $[\alpha\ \beta]$ is regulated based on image data. For example, in images with 8-bit precision, this bound is [0 255]. It means that the final restored image will be in the range of input image. In image restoration based on POCS, two convex sets including RAP-2D and LA are used in the restoration process. This procedure is followed by projection of restored image into hyperplanes as following:

$$f^{(k+1)} = P_{C_{RAP-2D}} P_{C_{LA}} \quad (10)$$

At each iteration, the image is projected first into RAP-2D using Equation (5). In this step, the qualification of the restoration is affected significantly by λ parameter which will be discussed in section 5. Afterward, $P_{C_{LA}}$ restrict the pixels values to be in the interval [0 255]. RAP-2D and LA projection are performed by $P_{C_{RAP-2D}}$ and $P_{C_{LA}}$ projection operators respectively [32].

3. PARTICLE SWARM OPTIMIZATION

Particle Swarm Optimization (PSO) [33] is a population-based meta-heuristic search optimization technique stem from the bird flocking behavior. The core of PSO is by the way that combine the global exploration and local exploitation strategies to find the optimum solution [34]. The main purpose of optimization problems is finding the optimum value of a cost function in D-dimensional space. In PSO, a population of particles is randomly initialized along the D-dimensional search space which each particle $p_i = (\vec{x}_i, \vec{v}_i) \in R^d$ is a point in this space with position $(\vec{x}_i)$ and velocity $(\vec{v}_i)$ properties. In the fist stage of the PSO, both position and velocity for all particles are randomly initialized. In the next step, each particle saves both the best position in its history as local optimum point and the best position among all particles as global optimum point. At each iteration, velocity and position of particles are updated as follows:

$$\vec{v}_i = w\vec{v}_i + c_1 r_1 (\hat{\vec{x}}_i - \vec{x}_i) + c_2 r_2 (\hat{\vec{s}} - \vec{x}_i) \quad (11)$$

$$\vec{x}_i = \vec{x}_i + \vec{v}_i \quad (12)$$

where $\hat{\vec{x}}_i$ and $\hat{\vec{s}}$ are respectively the local and global positions, w is the inertia weight, r_1 and r_2 are the random numbers in the interval [0 1] and finally c_1 and c_2 are the acceleration coefficients. Update equations show that particles follow the direction which is the combination of their current path, local and global paths [34].

4. PROPOSED POCS IMAGE RESTORATION BASED ON PSO

Relaxation parameter λ affect the result of POCS method in image restoration significantly. For declaring the effect of λ parameter, a sample image is blurred by Gaussian filter and then Gaussian noise is added to it. For different amounts of λs, POCS is applied to the image. The restored images results are shown in Figure 1 which shows that for the low amounts of λ, the restoration results are poor while by increasing the λ, although restored images are better visually, there are so many artifacts in high frequency regions of the image. This show that there is no any rule for expressing accuracy of the restoration results based on either increasing or decreasing the λ parameter.

With knowing the importance of λ parameter, empirical selection of this parameter is very difficult task since it is a variable in the continuous space. The main contribution of this paper is finding the optimal λ^* parameter which leads to the best restoration results. In this paper, a 1-dimensional continuous optimization algorithm is proposed which is an extension of classic PSO. In this optimization problem the cost function is the
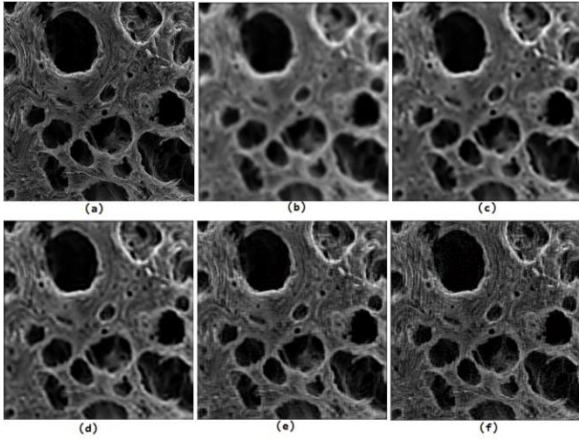
Figure 1. (a) Original image, (b) blurred and noised image, (c) restored image with $\lambda = 0.1$, (d) restored image with $\lambda = 1$, (e) restored image with $\lambda = 2.5$ and (f) restored image with $\lambda = 3.5$

accuracy of the restored image which must be maximized for the optimum solution λ^*. There are some measures for evaluating the restored image result. In this research we have used Improvement Signal to Noise Ratio (ISNR), Mean Absolute Error (MAE) and Mean Squared Error (MSE) measures which are computed as following:

$$ISNR = 10 \log_{10} \left(\frac{\sum_{i,j}[g(i,j)-f(i,j)]^2}{\sum_{i,j}[\hat{f}(i,j)-f(i,j)]^2} \right) \qquad (13)$$

$$MAE = \frac{\sum_{i,j}|\hat{f}(i,j)-f(i,j)|}{MN} \qquad (14)$$

$$MSE = \frac{\sum_{i,j}|\hat{f}(i,j)-f(i,j)|^2}{MN} \qquad (15)$$

where f, $\hat{f}$ and g are original image, restored image and degraded image respectively. Also, M and N are the image dimensions. It is worth mentioning that the higher amount of ISNR, the better restoration results are achieved while for MAE and MSE this relation is vice versa. Since our proposed algorithm maximize the above restoration measures, the cost functions for optimization problem are ISNR, $\frac{1}{MAE}$ and $\frac{1}{MSE}$.

In the optimization problem, each particle is a random number in the 1-dimensional search space which is the Lambda relaxation parameter. In the initial generation of particles, all particles are forced to be in the interval $[\lambda_{min}, \lambda_{max}]$ since there aren't appropriate restoration results for any amount of Lambda.

The velocity update is the core of PSO algorithm which is a sum of three parts include exploration, self-exploitation and social exploitation. The exploration part has inertia weight coefficient while self-exploitation and social exploitation have $c_1 r_1$ and $c_2 r_2$ coefficients respectively. In this paper the new schema for velocity update is proposed by the way that first particles are divided into two groups based on their fitness include the

first B percent of the best particles and remained 1-B percent of other particles named as group 1 and group 2 respectively. Then, velocity update rules are applied to particles groups separately.

Inertia weight has important role in controlling the process of exploration and exploitation. In this paper, we have proposed the new method for assigning particles inertia weight. It is clear that the higher amount of inertia weight, the more exploration of search space is occurred by particles. So, inertia weights for particles in group 1 are increased to accelerate their search towards the global optimum. On the other hand, particles in group 2 try to have a balance between exploration and exploitation. So, they decrease their weights linearly. This idea is stem from self-regulating PSO algorithm which applied the above rule only for the best particle [35]. The inertia weight strategy for particles is proposed to be defined as following:

$$w_i(t) = \begin{cases} w_i(t-1) + \Delta w \,, if \; particle \; is \; in \; group1 \\ w_i(t-1) - \Delta w, if \; particle \; is \; in \; group2 \end{cases} \qquad (16)$$

where $\Delta w = \frac{\eta}{IterationNumber}$ and η is a constant value.

For the self-exploitation and social exploitation, beside $c_1 r_1$ and $c_2 r_2$ two new coefficients are proposed as C_{se} and C_{So} respectively. In contrast with inertia weight, these two parts of velocity update rule highlight the exploitation property in the search space. As we mentioned in inertia weight rule, for the particles with the higher fitness, it is better that they have more ability for exploration of the search space rather than exploitation. So, for these particles we propose that their exploration weight be high in contrast with assigning the lower weights for exploitation. On the other hand, for other particles with lower fitness the exploitation property must be more highlighted since they must follow the direction of global and local particles to achieve the better fitness. Exploitation coefficients of the particles of group 1 and group 2 are defined as following:

$$C_{se}{}^{g1}(i) = \begin{cases} 1\,, & if \; a < P_1 \\ 0, & otherwise \end{cases} \qquad (17)$$

$$C_{so}{}^{g1}(i) = \begin{cases} 1\,, & if \; a < P_2 \\ 0, & otherwise \end{cases} \qquad (18)$$

$$C_{se}{}^{g2}(i) = \begin{cases} 1\,, & if \; a < P_3 \\ 0, & otherwise \end{cases} \qquad (19)$$

$$C_{so}{}^{g2}(i) = \begin{cases} 1\,, & if \; a < P_4 \\ 0, & otherwise \end{cases} \qquad (20)$$

These equations verify that particles with higher fitness update their velocity first based on their current direction as exploration of the search space, and second based on social exploitation and finally based on self-exploitation. For the particles with lower fitness this rule is implemented in equations vice versa. The flowchart of the proposed algorithm is depicted in Figure 2.
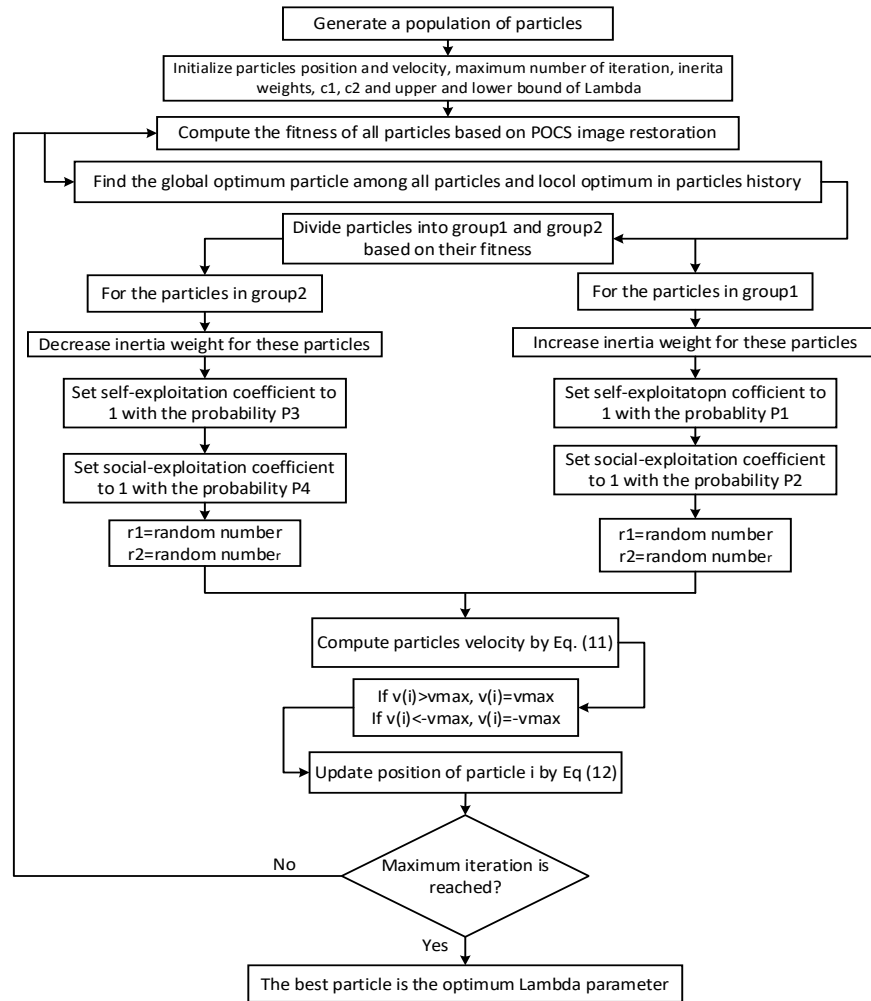
Figure 2. Flowchart of the proposed POS algorithm for finding optimum Lambda parameter

6. EXPERIMENTAL SETUP

To show the utility of the proposed algorithm a series of experiments is conducted. We implement our algorithm on a machine with 2.26 GHz Corei7 CPU and 6GB of RAM and windows 7. In these experiments, various parameter values were tested for PSO, POCS and our proposed optimization method in image restoration. According to our experiments, the highest performance is achieved by setting the parameters to values are shown in Table 1. For particles in group 1 with higher fitness, the self-exploitation and social exploitation considered in their velocity update with the probabilities of 0.3 and 0.6 respectively while these probabilities are both 0.8 for particles in group 2. Image restoration methods are evaluated on small number of well-known images. In this research, Cameraman, Fruits and Boats images are used for evaluation which is frequently used by image restoration researches.

TABLE 1. Parameter setting

Parameter	Value	Parameter	Value	Parameter	Value
Number of convex sets	20	C1 and C2	1	λ_{min}	-5
Maximum number of iterations	50	vmax	0.5	λ_{max}	+5
Number of particles	100	Initial weights	1.5	η	0.35
P1	0.3	P2	0.6	P3 and P4	0.8

6. EXPERIMENTAL RESULTS

To illustrate the effectiveness of proposed algorithm, it is evaluated by four measures Relative Error, ISNR, MSE and MAE. Three measures ISNR, MAE and MSE were defined previously in Equations (13)-(15) where they have been used as cost functions of PSO optimization. Relative error is defined as:

$$RelativeError(X) = \frac{\|\hat{X} - X\|_F}{\|\hat{X}\|_F} \tag{21}$$

where X is noised image, $\hat{X}$ is original noise-free image and $\|.\|_F$ is Frobenius norm.

The proposed method has been compared with 5 image restoration models which were proposed in [1, 7, 36-38]. To have variations in experiments, images are first blurred by blur matrix A which is Kronecker product of A_1 and A_2. These matrixes are calculated as following:

$$A_1(i,j) = A_2(i,j) = \begin{cases} \frac{1}{\sigma\sqrt{2\pi}} \exp\left(-\frac{(i-j)^2}{2\sigma^2}\right) & |i-j| \leq r \\ o & otherwise \end{cases} \tag{22}$$

In the first round of comparison, the proposed model is compared with PSO for three images and two noise sets (σ, r, NV) including $(4.4, 5, 2)$ and $(8.4, 7, 2.5)$. The proposed method has lower relative error, MAE and MSE; and higher INSR in all images and all noise sets compared with PSO (Table 2). It means that the proposed method outperforms PSO in all experiments and restores images with higher qualities.

Then, the white Gaussian noise of mean 0 and variance NV are added to blurred noise-free image. For this task 4 configurations for noise parameters (σ, r, NV) including $(1.4, 3, 1)$, $(4.4, 5, 2)$, $(8.4, 7, 2.5)$ and $(12.4, 10, 5)$ are used as noise sets 1, 2, 3 and 4, respectively.

Relative Error, ISNR, MSE and MAE of all methods for 4 noise sets are reported in Table 3. In relative error, the proposed method is the best method in Cameraman and Boats compared with all competitive models in which the best improvement of 24.93% was achieved in the last noise set 4. In Fruits, method by He et al. [1] outperforms all methods in all noise sets. With respect to ISNR, the proposed method achieves the highest results in Cameraman and Boats. Also, in the noise set 1, the proposed method has higher ISNR while in other noise sets [1] reaches to the best ISNRs. Promising results were achieved by the proposed method in MSE and MAE measures in which the proposed method is the best method in Cameraman and Boats while in Fruit image methods by Rashno et al. [38], Pang et al. [7] and He et al. [1] achieves lower values in different noise sets. The main conclusion from these experiments is that, the proposed method outperforms other methods in 32 cases out of 48 cases. Method proposed by He et al. [1] is the runner up model which is superior in 12 cases. Finally, methods developed by Rashno et al. [38] and Bouhamidi et al. [37] with 3 and 1 best cases are the third and fourth model, respectively.

As visual comparison, results of all models were shown for Boats and Fruits images in Figures 3 and 4, respectively. It is visually clear that the proposed restoration model restores images with better details.

7. COMPUTATIONAL COMPLEXITY OF FITNESS FUNCTION

During optimization process, restored images are compared with original images with respect to ISNR, MAE and MSE measures. For images with dimension $(M \times N)$, computational cost of ISNR is

TABLE 2. Comparison between PSO and the proposed model

		Cameraman		Fruits		Boats	
	σ	4.4	8.4	4.4	8.4	4.4	8.4
Noise Sets	r	5	7	5	7	5	7
	NV	2	2.5	2	2.5	2	2.5
Relative Error	PSO	0.2312	0.0352	**0.2721**	**0.3318**	0.2231	0.2728
	Proposed	**0.2045**	**0.0315**	0.2481	0.3247	**0.1910**	**0.2548**
ISNR	PSO	0.0332	0.0110	**0.0382**	**0.0141**	0.0404	0.0122
	Proposed	**0.0415**	**0.0142**	0.0412	0.0168	**0.0442**	**0.0157**
MAE	PSO	7.3425	11.562	9.4560	13.878	10.122	11.342
	Proposed	**6.2549**	**9.2548**	**8.2549**	12.548	8.4587	**9.7854**
MSE	PSO	125.30	154.80	**139.10**	186.20	129.10	154.10
	Proposed	**120.50**	**142.80**	136.30	171.50	**124.10**	**145.50**

TABLE 3. Relative Error, ISNR, MSE and MAE of all methods for 4 noise sets

		Cameraman				Fruits				Boats			
	σ	1.4	4.4	8.4	12.4	1.4	4.4	8.4	12.4	1.4	4.4	8.4	12.4
	r	3	5	7	10	3	5	7	10	3	5	7	10
	NV	1	2	2.5	5	1	2	2.5	5	1	2	2.5	5
Relative Error	[36]	0.2065	0.2712	0.3283	0.5521	0.2354	0.2914	0.3467	0.4976	0.2147	0.2747	0.3157	0.4454
	[37]	0.1812	0.2634	0.3294	0.4834	0.2059	0.2848	0.3387	0.4453	0.1812	0.2798	0.3074	0.4056
	[38]	0.1831	0.2418	0.3243	0.4154	0.2123	0.2534	0.3341	0.3918	0.1956	0.2647	0.3086	0.3642
	[7]	0.1748	0.2315	0.0314	0.03514	0.2045	0.2457	0.3215	0.3854	0.1984	0.2214	0.2952	0.3547
	[1]	0.1758	0.2218	0.03215	0.03418	**0.2018**	**0.2348**	**0.3158**	**0.3315**	0.1874	0.2098	0.2857	0.3425
	Proposed	**0.1711**	**0.2045**	**0.03154**	**0.03028**	0.2084	0.2481	0.3247	0.3718	**0.1798**	**0.191**	**0.2548**	**0.3025**
ISNR	[36]	0.0432	0.0301	0.0104	-0.024	0.0382	0.0312	0.0091	-0.161	0.0357	0.0301	0.0084	-0.141
	[37]	0.0541	0.0304	0.0113	-0.073	0.0443	0.0356	0.0112	-0.067	0.0414	0.0325	0.0101	-0.054
	[38]	0.0514	0.0332	0.0118	-0.013	0.0412	0.0402	0.0184	-0.034	0.0401	0.0385	0.0136	-0.036
	[7]	0.0548	0.0321	0.0114	-0.025	0.0457	0.0451	0.0154	-0.031	0.0422	0.0418	0.0122	-0.029
	[1]	0.0568	0.0347	0.0121	-0.034	0.0469	**0.0445**	**0.0175**	**-0.033**	0.0435	0.0424	0.0141	-0.034
	Proposed	**0.0598**	**0.0415**	**0.0142**	**-0.026**	**0.0498**	0.0412	0.0168	-0.039	**0.0468**	**0.0442**	**0.0157**	**-0.022**
MAE	[36]	7.9786	10.873	14.653	28.873	8.8753	11.8912	14.874	25.543	6.1452	9.4456	12.452	21.475
	[37]	7.0134	10.234	13.873	21.453	7.9853	11.1546	14.165	18.843	6.4856	9.4562	11.475	19.365
	[38]	7.3421	9.1245	13.465	17.764	8.4633	10.1342	13.756	**16.345**	5.4253	9.7452	11.756	16.458
	[7]	7.5484	8.1256	12.548	17.256	7.2549	9.2548	**12.251**	19.254	5.7458	**8.1246**	10.785	16.485
	[1]	6.6589	7.1247	11.254	**14.254**	**7.2548**	9.2546	12.254	18.548	5.2154	8.4567	10.149	15.475
	Proposed	**6.1258**	**6.2549**	**9.2548**	15.254	7.4458	**8.2549**	12.548	19.541	**4.4785**	8.4587	**9.7854**	**13.456**
MSE	[36]	125.7	149.3	174.5	213.5	135.1	153.2	179.7	221.2	133.5	152.1	168.5	215.5
	[37]	118.3	141.9	168.6	205.3	125.6	146.4	172.1	209.9	120.7	142.5	165.7	201.9
	[38]	121.4	135.5	161.5	191.4	127.3	139.7	165.6	200.3	122.6	140.4	160.4	198.7
	[7]	120.2	129.2	160.5	182.6	125.6	135.4	**160.5**	186.3	121.1	140.6	154.3	192.1
	[1]	119.2	126.5	151.7	180.5	**124.8**	**133.5**	166.7	**185.2**	119.8	128.2	157.4	186.6
	Proposed	**111.2**	**120.5**	**142.8**	**152.7**	125.9	136.3	171.5	188.5	**115.4**	**124.1**	**145.5**	**174.1**

equivalent with by the following parameters:

$$ISNR \cong \left(\frac{\sum_{i=1}^{M}\sum_{j=1}^{N}[g(i,j)-f(i,j)]^2}{\sum_{i=1}^{M}\sum_{j=1}^{N}[\hat{f}(i,j)-f(i,j)]^2} \right) \qquad (23)$$

There are $(M \times N)$ subtractin operations and $(M \times N)$ square operations, and 1 addition operation, the total $(M \times N) + (M \times N) + 1$ operations in numerator and denominator. Therefore, $2[(M \times N) + (M \times N) + 1] + 1$ operations are needed for ISNR computation. By the same way, for MAE and MSE, $[(M \times N) + (M \times N) + 1] + 2$ operations are needed.

$$MAE \cong \left(\frac{\sum_{i=1}^{M}\sum_{j=1}^{N}|\hat{f}(i,j)-f(i,j)|}{MN} \right) \qquad (24)$$

$$MSE \cong \left(\frac{\sum_{i=1}^{M}\sum_{j=1}^{N}(\hat{f}(i,j)-f(i,j))^2}{MN} \right) \qquad (25)$$

Since ISNR, MAE and MSE are used simultaneously as fitness function for particle evaluation, totally $6(M \times N) + 9$ Operations are needed for finness cmputation which is in complexity O(MN).

8. CONCLUSION

An image restoration model was presented by projection onto convex sets (POCS) and particle swarm optimization (PSO). Images were projected during restoration process and relaxation parameter was optimized by PSO. The proposed model was evaluated in several cases of images with different noise sets. Restored images were assessed by four criteria including Relative Error, ISNR, MSE and MAE which showed that
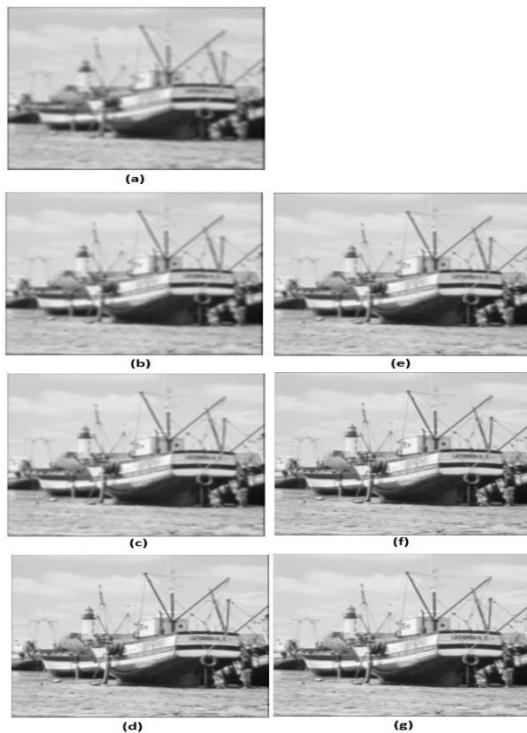
Figure 3. (a) Blurred and noised image, (b) restored image by [36], (c) restored image by [37], (d) restored image by [38], (e) restored image by [7], (f) restored image by [1], and (g) restored image by the proposed method
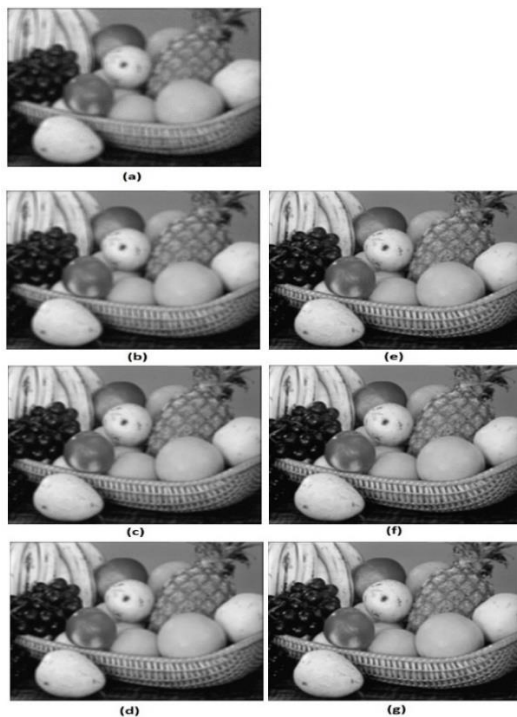
Figure 4. (a) Blurred and noised image, (b) restored image by [36], (c) restored image by [37], (d) restored image by [38], (e) restored image by [7], (f) restored image by [1], and (g) restored image by the proposed method

the proposed method is the best method among competitive methods. Suggested works will be directed to optimize more parameters of POCS by optimization methods. Finally, developing proposed restoration model for other noise types can be proposed as another future work.

9. REFERENCES

1.   He, L., Wang, Y., Liu, J., Wang, C., and Gao, S., "Single image restoration through ℓ2-relaxed truncated ℓ0 analysis-based sparse optimization in tight frames", *Neurocomputing*, Vol. 443, (2021), 272-291, doi: 10.1016/j.neucom.2021.02.053.

2.   Li, Y., Xia, Q., Lee, C., Kim, S., and Kim, J., "A robust and efficient fingerprint image restoration method based on a phase-field model", *Pattern Recognition*, Vol. 123, (2022), 108405, doi: 10.1016/j.patcog.2021.108405.

3.   Kishore, A., Kumar, A., and Dang, N., "Enhanced image restoration by GANs using game theory", *Procedia Computer Science*, Vol. 173, (2020), 225-233, doi: 10.1016/j.procs.2020.06.027.

4.   Cao, J., and Wu, J., "A conjugate gradient algorithm and its applications in image restoration", *Applied Numerical Mathematics*, Vol. 152, (2020), 243-252, doi: 10.1016/j.apnum.2019.12.002.

5.   Deng, X., and Dragotti, P. L., "Deep convolutional neural network for multi-modal image restoration and fusion", *IEEE Transactions on Pattern Analysis and Machine Intelligence*, Vol. 43, No. 10, (2020), 3333-3348, doi: 10.1109/TPAMI.2020.2984244.

6.   Papyan, V., and Elad, M., "Multi-scale patch-based image restoration", *IEEE Transactions on Image Processing*, Vol. 25, No. 1, (2015), 249-261, doi: 10.1109/TIP.2015.2499698.

7.   Pang, Z. F., Guo, L. Z., Duan, Y., and Lu, J., "Image restoration based on the minimized surface regularization", *Computers & Mathematics with Applications*, Vol. 76, No. 8, (2018), 1893-1905, doi: 10.1016/j.camwa.2018.07.037.

8.   Rudin, L. I., Osher, S., and Fatemi, E., "Nonlinear total variation based noise removal algorithms", *Physica D: Nonlinear Phenomena*, Vol. 60, No. 1-4, (1992), 259-268, doi: 10.1016/0167-2789(92)90242-F.

9.   Zhi, X., Jiang, S., Zhang, L., Hu, J., Yu, L., Song, X., and Gong, J., "Multi-frame image restoration method for novel rotating synthetic aperture imaging system", *Results in Physics*, Vol. 23, (2021), 103991, doi: 10.1016/j.rinp.2021.103991.

10. Zhang, Y. "An EM-and wavelet-based multi-band image restoration approach", In 2014 19th International Conference on Digital Signal Processing, (2014), 617-620, doi: 10.1109/ICDSP.2014.6900738.

11. Tanikawa, R., Fujisawa, T., and Ikehara, M., "Image restoration based on weighted average of multiple blurred and noisy images", In 2018 International Workshop on Advanced Image Technology (IWAIT), (2018), 1-4, doi: 10.1109/IWAIT.2018.8369665.

12. Ševčík, J., Šmídl, V., and Šroubek, F., "A n adaptive correlated image prior for image restoration problems", *IEEE Signal Processing Letters*, Vol. 25, No. 7, (2018), 1024-1028, doi: 10.1109/LSP.2018.2836964.

13. Hu, T., Li, W., Liu, N., Tao, R., Zhang, F., and Scheunders, P., "Hyperspectral image restoration using adaptive anisotropy total variation and nuclear norms", *IEEE Transactions on Geoscience and Remote Sensing*, Vol. 59, No. 2, (2020), 1516-1533, doi: 10.1109/TGRS.2020.2999634.

14. Dar, Y., Elad, M., and Bruckstein, A. M., "Restoration by compression", *IEEE Transactions on Signal Processing*, Vol. 66, No. 22, (2018), 5833-5847, doi: 10.1109/TSP.2018.2871388.

15. Li, X. Q., Fang, K. L., and Jin, C., "Super-Resolution Restoration for Image Based on Entropy Constraint and Projection onto Convex Set", *In Advanced Materials Research*, Vol. 468, (2012), 1041-1048, doi: 10.4028/www.scientific.net/AMR.468-471.1041.

16. Lu, H., Li, S., Liu, Q., and Zhang, M., "MF-LRTC: Multi-filters guided low-rank tensor coding for image restoration", *Neurocomputing*, Vol. 303, (2018), 88-102, doi: 10.1016/j.neucom.2018.04.046.

17. Choi, J. K., Dong, B., and Zhang, X., "An edge driven wavelet frame model for image restoration", *Applied and Computational Harmonic Analysis*, Vol. 48, No. 3, (2020), 993-1029, doi: 10.1016/j.acha.2018.09.007.

18. Motohashi, S., Nagata, T., Goto, T., Aoki, R., and Chen, H., "A study on blind image restoration of blurred images using R-map", In 2018 International Workshop on Advanced Image Technology (IWAIT), 1-4, 2018, doi: 10.1109/IWAIT.2018.8369650.

19. Liu, Z., Yu, L., and Sun, H., "Image restoration via Bayesian dictionary learning with nonlocal structured beta process", *Journal of Visual Communication and Image Representation*, Vol. 52, (2018), 159-169, doi: 10.1016/j.jvcir.2018.02.011.

20. Gou, Y., Li, B., Liu, Z., Yang, S., and Peng, X., "Clearer: Multi-scale neural architecture search for image restoration", *Advances in Neural Information Processing Systems*, Vol. 33, (2020), 17129-17140, doi: 10.48550/arXiv.2203.04313.

21. Xia, X., Xing, Y., Wei, B., Zhang, Y., Li, X., Deng, X., and Gui, L., "A fitness-based multi-role particle swarm optimization", *Swarm and Evolutionary Computation*, Vol. 44, (2019), 349-364, doi: 10.1016/j.swevo.2018.04.006.

22. Mehmood, Y., Sadiq, M., Shahzad, W., and Amin, F., "Fitness-based acceleration coefficients to enhance the convergence speed of novel binary particle swarm optimization", In 2018 International Conference on Frontiers of Information Technology (FIT), 355-360, 2018, doi: 10.1109/FIT.2018.00069.

23. Iravani, S., and Ezoji, M., "A General Framework for 1-D Histogram-based Image Contrast Enhancement", *International Journal of Engineering, Transactions A: Basics*, Vol. 29, No. 10. (2016), 1384-1391, doi: 10.5829/idosi.ije.2016.29.10a.09.

24. Tang, R., Zhou, X., and Wang, D., "Improved Adaptive Median Filter Algorithm for Removing Impulse Noise from Grayscale Images", *International Journal of Engineering, Transactions A: Basics*, Vol. 30, No. 10, (2017), 1503-1509, doi: 10.5829/ije.2017.30.10a.11.

25. Lin, L., and Feng, L., "Comparative Analysis of Image Denoising Methods Based on Wavelet Transform and Threshold Functions", *International Journal of Engineering, Transactions B: Applications*, Vol. 30, No. 2, (2017), 199-206, doi: 10.5829/idosi.ije.2017.30.02b.06.

26. Mortezaei, Z., Hassanpour, H., and Asadi Amiri, S., "Image Enhancement Using an Adaptive Un-sharp Masking Method Considering the Gradient Variation", *International Journal of Engineering, Transactions B: Applications*, Vol. 30, No. 8, (2017), 1118-1125, doi: 10.5829/ije.2017.30.08b.02.

27. Azari Nasrabad, F., Hassanpour, H., and Asadi Amiri, S, "Adaptive Image Dehazing via Improving Dark Channel Prior", *International Journal of Engineering, Transactions B: Applications*, Vol. 32, No. 2, (2019), 249-255, doi: 10.5829/ije.2019.32.02b.10.

28. Seyyedyazdi, S. J., and Hassanpour, H., "Improving Super-resolution Techniques via Employing Blurriness Information of the Image", *International Journal of Engineering, Transactions B: Applications*, Vol. 31, No. 2, (2018), 241-249, doi: 10.5829/ije.2018.31.02b.07.

29. Seyyedyazdi, S. J., and Hassanpour, H., "Super-resolution of Defocus Blurred Images", *International Journal of Engineering, Transactions A: Basics*, Vol. 33, No. 4, (2020), 539-545, doi: 10.5829/ije.2020.33.04a.04.

30. Mammone, R. J., "Computational methods of signal recovery and recognition", *John Wiley & Sons, Inc*., (1992), ISBN-13: 978-0471853848.

31. Kuo, S. S., and Mammone, R. J., "Image restoration by convex projections using adaptive constraints and the L/sub 1/norm", *IEEE Transactions on Signal Processing*, Vol. 40, No. 1, (1992), 159-168, doi: 10.1109/78.157191.

32. Papa, J. P., Fonseca, L. M., and de Carvalho, L. A., "Projections onto convex sets through particle swarm optimization and its application for remote sensing image restoration", *Pattern Recognition Letters*, Vol. 31, No. 13, (2010), 1876-1886, doi: 10.1016/j.patrec.2010.02.012.

33. Kennedy, J., and Eberhart, R., "Particle swarm optimization", In Proceedings of ICNN'95-international conference on neural networks, Vol. 4, (1995), 1942-1948, doi: 10.1109/ICNN.1995.488968.

34. Eberhart, R. C., Shi, Y., and Kennedy, J. "Swarm intelligence", *Elsevier*, (2001), ISBN: 9781498741071.

35. Tanweer, M. R., Suresh, S., and Sundararajan, N., "Self-regulating particle swarm optimization algorithm", *Information Sciences*, Vol. 294, (2015), 182-202, doi: 10.1016/j.ins.2014.09.053.

36. B. Morini, M. Porcelli, and R. Chan, "A reduced Newton method for constrained linear least-squares problems", *Journal of Computational and Applied Mathematics*, Vol. 233, 2200–2212, 2010, doi: 10.1016/j.cam.2009.10.006.

37. Bouhamidi, Abderrahman, Rentsen Enkhbat, and Khalide Jbilou. "Conditional gradient Tikhonov method for a convex optimization problem in image restoration", *Journal of Computational and Applied Mathematics*, Vol. 255, (2014), 580-592, doi: 10.1016/j.cam.2013.06.011.

38. Rashno, Abdolreza, Foroogh Sadat Tabataba, and Saeed Sadri. "Image restoration with regularization convex optimization approach", *Journal of Electrical Systems and Signals*, Vol. 2, No. 2, (2014), 32-36, doi: 10.48550/arXiv.1902.02059.

Persian Abstract

چکیده

ترمیم تصویر عبارت است از به دست آوردن یک تصویر باکیفیت از تصویر نویزی یا خراب‌شده که در کاربردهای زیادی از جمله در MRI و تشخیص اثر انگشت استفاده می‌شود. در این مقاله یک مدل ترمیم تصویر مبتنی بر نگاشت بر مجموعه‌های محدب (POCS)و بهینه‌سازی ازدحام ذرات (PSO) ارائه شده است. برای این منظور، تعدادی مجموعه محدب به عنوان محدودیت‌ها استفاده شده و تصویر به این مجموعه نگاشت می‌شود تا تصویر ترمیم شده حاصل شود. از آنجاییکه پارامتر ریلکسیشن در POCS تاثیر بسزایی در نتایج ترمیم تصویر دارد برای تعیین مقدار بهینه‌ی آن از الگوریتم PSO استفاده شده است. روش پیشنهادی روی ۳ تصویر مشهور در چهار نویز مختلف پیاده‌سازی شده و با ۵ روش ترمیم تصویر مقایسه شده است. نتایج نشان می‌دهند که بر اساس معیارهای RelativeError، ISNR، MAE و MSE، مدل پیشنهادی در ۳۲ حالت از ۴۸ حالت بهتر از دیگر مدل‌ها بوده است.